Iron overload: accuracy of in-phase and out-of-phase MRI as a quick method to evaluate liver iron load in haematological malignancies and chronic liver disease

J M VIRTANEN, MD, T K PUDAS, MD, J A RATILAINEN, MD, J P SAUNAVAARA, MSc, PhD, M E KOMU, MSc, PhD and R K PARKKOLA, MD, PhD

Department of Radiology, Medical Imaging Centre of Southwest Finland, Turku University Hospital, Turku, Finland

Objectives: The purpose of this prospective study was to evaluate the accuracy of in-phase and out-of-phase imaging to assess hepatic iron concentration in patients with haematological malignancies and chronic liver disease.
Methods: MRI-based hepatic iron concentration (M-HIC, $\mu mol\,g^{-1}$) was used as a reference standard. 42 patients suspected of having iron overload and 12 control subjects underwent 1.5 T in- and out-of-phase and M-HIC liver imaging. Two methods, semi-quantitative visual grading made by two independent readers and quantitative relative signal intensity (rSI) grading from the signal intensity differences of in-phase and out-of-phase images, were used. Statistical analyses were performed using the Spearman and Kruskal–Wallis tests, receiver operator curves and κ coefficients.
Results: The correlations between M-HIC and visual gradings of Reader 1 ($r=0.9534$, $p<0.0001$) and Reader 2 ($r=0.9456$, $p<0.0001$) were higher than the correlations of the rSI method ($r=0.7719$, $p<0.0001$). There was excellent agreement between the readers (weighted $\kappa=0.9619$). Both visual grading and rSI were similar in detecting liver iron overload: rSI had 84.85% sensitivity and 100% specificity; visual grading had 85% sensitivity and 100% specificity. The differences between the grades of visual grading were significant ($p<0.0001$) and the method was able to distinguish different degrees of iron overload at the threshold of 151 $\mu mol\,g^{-1}$ with 100% positive predictive value and negative predictive value.
Conclusion: Detection and grading of liver iron can be performed reliably with in-phase and out-of-phase imaging. Liver fat is a potential pitfall, which limits the use of rSI.

Received 17 July 2010
Revised 1 November 2010
Accepted 10 November 2010

DOI: 10.1259/bjr/22327146

Iron overload is a clinically recognised condition with variety of aetiologies and clinical manifestations [1–4]. Liver iron concentration correlates closely with the total body iron stores [5]. The excess iron accumulates mainly in the liver and the progressive accumulation of toxic iron can lead to organ failure if untreated [2, 4]. Several diseases causing iron overload, such as transfusion-dependent anaemia, haematological malignancies, thalassaemia, haemochromatosis and chronic liver disease, result in a large number of patients with a potentially treatable iron overload [1, 2, 4].

Several quantitative MRI methods for iron overload measurement by multiple sequences have been established, such as proportional signal intensity (SI) methods and proton transverse relaxation rates (R_2, R_2*) [4, 6, 7]. A gradient echo liver-to-muscle SI-based algorithm [8] has been widely validated and used for quantitative liver iron measurement [8–11]. MRI-based hepatic iron concentration (M-HIC, $\mu mol\,g^{-1}$ liver dry weight) with corresponding R_2* [9] can be calculated with this method which is a directly proportional linear iron indicator, virtually independent of the fat fraction, as the echo times are taken in-phase [8, 9]. This method showed a high accuracy in calibrations with the biochemical analysis of liver biopsies (3–375 $\mu mol\,g^{-1}$) of 174 patients. The mean difference of 0.8 $\mu mol\,g^{-1}$ (95% confidence interval of –6.3 to 7.9) between this method and the biochemical analysis is quite similar [8] to the intra-individual variability found in histological samples [12].

The quantitative MRI methods are based on progressive SI decay, with the longer echo times due to relaxing properties of iron. Interestingly, this iron-induced effect is seen in MR images with multiple echoes [4, 6–11], but also in dual-echo images, namely in-phase and out-of-phase imaging [13, 14]. In-phase and out-of-phase imaging has become a routine part of liver MRI, performed initially for liver fat detection [6, 13, 15]. Quite recently some investigators have noticed an alternative approach of the sequence to detect liver iron overload due to the more pronounced SI decrease on in-phase images with the longer echo time [13, 14]. Yet, to our knowledge, this is the first prospective study evaluating the accuracy of in-phase and out-of-phase imaging to assess hepatic iron concentration.

The purpose of the study was to evaluate the capability and accuracy of dual-echo in-phase and out-of-phase imaging to assess hepatic iron concentration at

Address correspondence to: Dr Johanna Virtanen, Department of Radiology, Medical Imaging Centre of Southwest Finland, Turku University Hospital, Kiinamyllynkatu 4-8, PO Box 52, 20520 Turku, Finland. E-mail: jomavirtanen@dnainternet.net

1.5 T in patients with haematological malignancies and chronic liver disease. MRI-based hepatic iron concentration (M-HIC, μmol g^{-1}) was used as a reference standard [8, 9].

Methods and materials

Study subjects

This prospective, single centre study was conducted according to the Declaration of Helsinki guidelines. Written informed consent was obtained from all patients and healthy control subjects. The study protocol was approved by the local ethics committee. Patients with clinically suspected iron overload were recruited by haematologists at the Department of Medicine of Turku University Hospital over a 2 year period. A total of 54 subjects were taken into this study, which consisted of 42 patients and 12 controls. The diagnoses of all 42 patients consisted of haematological malignancies (n=26), aplastic anaemia (n=3), hereditary haemochromatosis (n=2), anaemia not otherwise specified (n=1), non-immunological haemolysis (n=1) and chronic liver diseases (n=9) including fatty liver disease, cirrhosis and alcoholic hepatic insufficiency. The diagnoses of the study group reflected the variety of the aetiologies of iron overload in our clinical context. The mean age of patients was 48.9 ± 12.5 years and that of controls was 41.3 ± 15.6 years. There was no significant difference between the mean ages (p=0.138) of patients and controls. The inclusion criteria for the patients was a clinically suspected iron overload due to either (1) red blood cell transfusions or (2) liver-affecting disease with elevated serum ferritin levels. Exclusion criterion was age under 18 years.

MRI

MR images were obtained using two superconducting 1.5 T MRI scanners with integrated body coil, spine and body matrix receiving surface coils. 37 study subjects were scanned using a Siemens Magnetom Symphony (Siemens Medical Solutions, Erlangen, Germany) and 17 subjects using a Siemens Magnetom Avanto scanner. Patients were instructed to fast 4 h before the MR examination. The imaging protocol consisted of the reference standard (M-HIC) [8, 9] and in-phase and out-of-phase imaging. The in-phase and out-of-phase imaging was obtained twice in a subgroup of 19 patients with both scanners. The mean interval of the two examinations at different scanners was 1.0 ± 2.5 days; range, 0–8 days.

The M-HIC imaging was performed according to the technique previously described [8, 9] and consisted of five gradient echo sequences [repetition time (TR), 120 ms; echo times (TEs), 4, 9, 14 and 21 ms; flip angle, 20°; and TR, 120 ms; TE, 4 ms; flip angle, 90°], obtained with body coil during breath-hold. Transverse T_1 weighted dual-echo in-phase and out-of-phase images of the liver were obtained with body coil during breath-hold using a spoiled gradient recalled echo sequence (TR, 168 ms; TE, 2.38 ms out-of-phase; TE, 4.76 ms in-phase; flip angle, 70°; slice thickness, 10 mm; matrix size, 146 × 256; field of view of 400 mm; time of acquisition, 25 s).

Image analysis and data collection

Image analysis was performed on a Siemens Syngo Multimodality Workplace (Siemens Medical Solutions).

For the reference standard, three mean signal intensities of regions of interests were obtained from each of the five different gradient echo sequences in each patient. R_2* and corresponding M-HIC were then analysed with the range of M-HIC between 5 and 320 μmol g^{-1} liver dry weight (n=48) according to the prior standardisation of scanner-specific differences [8, 9]. M-HIC values (n=6) at or above the upper limit (≥320 μmol g^{-1}) of the quantitative range were excluded from the correlation analysis. The upper limit of normal liver iron concentration was 36 μmol g^{-1} [4, 8, 9].

The visual grading method of in-phase and out-of-phase imaging was applied to evaluate the degree of iron overload semi-quantitatively in the study patients (n=42) using the criteria presented (Table 1). The images were analysed by two blinded, independent radiologists, Reader 1 (2 years of expertise in abdominal radiology) and Reader 2 (3 years of expertise in musculoskeletal radiology). They had no prior information of patients' clinical history, laboratory findings or iron status. The M-HIC >320 μmol g^{-1} values were set at 325 μmol g^{-1} in order to explore the visual grading method, including for the most severe iron-overloaded patients. The radiologists classified the patients into four grades (Figure 1) according to the visual criteria presented. The readers were instructed to emphasise in-phase criteria, especially if the readers suspected fatty liver disease based on out-of-phase images.

The relative signal intensity (rSI) difference (n=54) on in-phase and out-of-phase imaging was calculated as

$$\mathrm{rSI} = \frac{\mathrm{SI(out)} - \mathrm{SI(in)}}{\mathrm{SI(out)}} \times 100\% \qquad (1)$$

where SI(out) is signal intensity of out-of-phase and SI(in) is the signal intensity of in-phase images. This index was applied as a potential continuous iron indicator to test whether there was a more pronounced iron relaxation effect and signal decrease found on SI(in) with the longer echo time. The SI difference between out-phase and in-phase was calculated by subtraction of the whole liver as SI(out) minus SI(in). The most homogeneous slice of the subtracted sequence was chosen for measurements. Three regions of interest (Figure 1) with an area of 100–200 mm^2 were obtained from subtracted images from the axial slice at the right part of the right liver lobe, avoiding vessels and possible artefacts. SI(out) was measured separately from the same region of interest. The rSI difference of three regions of interest and the average rSI were calculated for each subject. If there was no signal in the subtracted images the SI difference was calculated additionally as SI(in) minus SI(out) to detect fatty liver, if present.

Statistical analysis

Statistical tests were performed using computer software GraphPad Prism version 5.00, 5.02, InStat version 3.05 (GraphPad Software, Inc., San Diego, CA) and SAS System for Windows, version 9.2 (SAS Institute Inc, Cary, NC).

Table 1. The criteria of visual grading method to assess the degree of liver iron overload

Grade	Description	Criteria	
		In-phase images	In-phase and out-of-phase images
0	Normal iron concentration	Liver signal intensity (SI) is greater than muscle SI	Liver SI of in-phase images and out-of-phase images is about the same
1	Minor iron overload	Liver SI is about as low as muscle SI	Liver SI of in-phase images is slightly lower than out-of-phase images
2	Moderate iron overload	Liver SI is lower than muscle SI, although not as low as the background noise	Liver SI of in-phase images is clearly lower than out-of-phase images
3	Severe iron overload	Liver SI is lower than muscle SI, and about as low as background noise	Liver SI of in-phase images is clearly lower than in out-of-phase images

Spearman rank correlation coefficients (r) with two-tailed p-values were used to evaluate all the correlations. The scatter plots were obtained using least square measures linear regression analysis. Paired t-tests with two-tailed p-values were used to express the ages of patients and controls and rSI values of different scanners with means $\pm$ standard deviation. The Kruskal–Wallis test was used to evaluate the differences between the grades of the visual grading method. The receiver operator characteristic (ROC) curve was applied to search for the optimal threshold for the rSI difference method of detecting iron overload. The sensitivity, specificity, positive predictive value (PPV), negative predictive value (NPV) and accuracy (%) of the methods for detecting liver iron overload were measured. The agreement between the readers was evaluated with the weighted κ coefficient.

Results

Liver iron overload was found in 27 of the 29 haematological patients (93%) and in 33 of all 42 patients

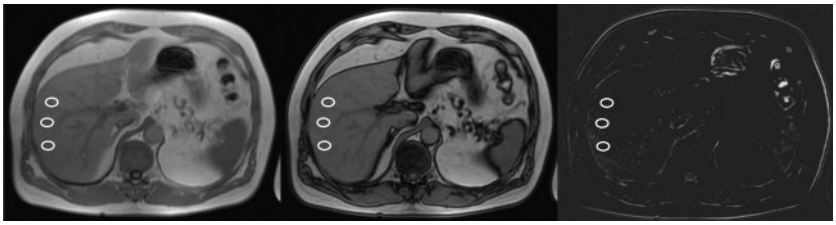

(a)

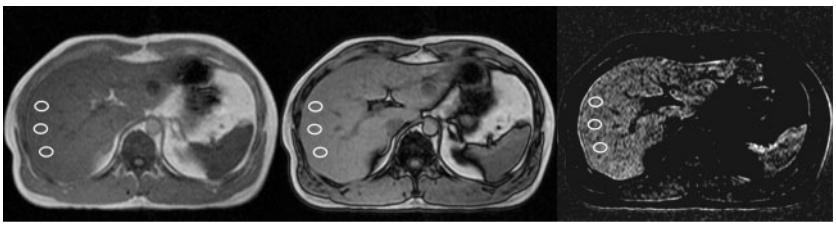

(b)

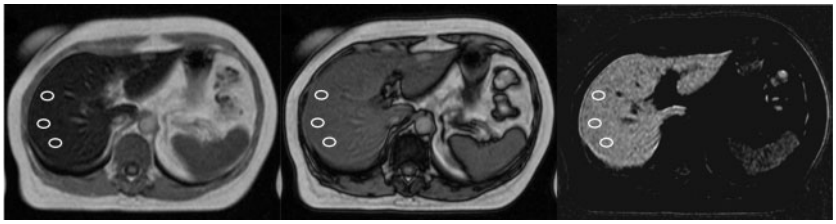

(c)

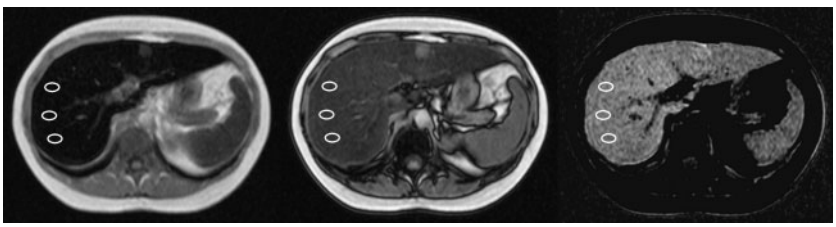

(d)

Figure 1. T_1 weighted axial in-phase and out-of-phase images demonstrating the criteria of visual grading and measurements of relative signal intensity (rSI) difference method in four patients as examples of different grades of iron overload. Three regions of interests were obtained for the rSI analysis. Left, in-phase image; middle, out-of-phase image; right, subtracted image calculated as the signal intensity of the in-phase image minus the signal intensity of the out-of-phase image. (a) Normal iron concentration (Grade 0) with MRI-based hepatic iron concentration (M-HIC) of 33 μmol g^{-1}. (b) Minor iron overload (Grade 1) with M-HIC of 115 μmol g^{-1}. (c) Moderate iron overload (Grade 2) with M-HIC of 193 μmol g^{-1}. (d) Severe iron overload (Grade 3) with M-HIC of 271 μmol g^{-1}.

(79%). 9 patients had a minor overload between 36 and 100 μmol g^{-1}, 12 patients had liver iron concentrations between 100 and 200 μmol g^{-1} and 12 had concentrations above 200 μmol g^{-1}. Among these, 6 patients had liver iron concentrations at or above 320 μmol g^{-1}. All of the 12 healthy controls had normal liver iron concentrations with a mean concentration of 12.8 ± 4.6 μmol g^{-1}.

Both the semi-quantitative visual grading and quantitative relative SI difference correlated very significantly with M-HIC. The correlation of visual gradings by Reader 1 ($r=0.9534$, $p<0.0001$) and Reader 2 ($r=0.9456$, $p<0.0001$) were higher than the correlation of the relative SI difference method ($r=0.7719$, $p<0.0001$). The best-fit values of the rSI method are demonstrated with linear fit:

$$\mathrm{M-HIC} = 3.562 \times \mathrm{rSI} + 26.99 \quad (2)$$

The visual grading method classified the study population into four grades (Figure 1, Table 1) of different degrees of iron accumulation. The differences between the medians of the grades (Table 2) were significant ($p<0.0001$) and the agreement between readers on visual grading was excellent (weighted $\kappa=0.9619$). Visual grading of both readers detected liver iron overload evaluated as Grades 1–3 with sensitivity of 85% [95% confidence interval (CI): 74–92%], specificity of 100% (95% CI: 81–100%), PPV of 100% (95% CI: 94–100%), NPV of 64% (95% CI: 44–81%), and accuracy of 88%. Interestingly, Grades 2 and 3 as a group were very accurate in finding moderate to severe liver iron overload of over 151 μmol g^{-1} with a sensitivity and PPV of 100% (95% CI: 91–100%) and a specificity and NPV of 100% (95% CI: 92–100%).

The optimal threshold of rSI difference method to detect iron overload was set at 10% to reach the best possible sensitivity of 85% (95% CI 68–95%) and specificity of 100% (95% CI 84–100%), PPV of 100% (95% CI 88–100%), NPV of 81% (95% CI 61–93%) and accuracy of 91%. The accuracy of rSI to detect liver iron overload at this threshold was evaluated using the ROC curve (area under the curve: 0.91; $p<0.0001$) and contingency table (Table 3): three out of five false-negative results were explained with detectable liver steatosis [SI(out)<SI(in)], which decreased the sensitivity of rSI. There was no significant difference between the rSI values from the different scanners ($n=19$, $p=0.675$). The mean of the difference was 0.005 ± 0.051.

Seven subjects showed detectable liver fat content at in-phase and out-of-phase imaging [SI(out)<SI(in)] with mean M-HIC values of 45.7 ± 45.3 μmol g^{-1}, range 10.4–140 μmol g^{-1}. Three patients showing both elevated liver fat and iron content were diagnosed as non-immunological haemolysis ($n=1$, M-HIC=140 μmol g^{-1}, Grade 1 of visual grading) and fatty liver disease with minor secondary haemosiderosis ($n=2$, M-HIC= 62 μmol g^{-1} and 43 μmol g^{-1}, Grade 0 of visual grading). The correlation between SI loss on out-of-phase images and M-HIC ($n=7$) was not significant ($r=0.6071$, $p=0.1667$).

Discussion

The aim of this study was to evaluate the capability of a clinically widely used in-phase and out-of-phase sequence as an iron indicator at 1.5 T. Although the in-phase and out-of-phase sequences were not optimised for iron quantification, our results indicate that the double echo approach of this sequence is of value as a quick method to estimate liver iron concentrations. Visual grading was found to be a feasible semi-quantitative method to evaluate the different degrees of liver iron overload, while the rSI difference method is more detailed as a continuous index.

Based on our results, the detection of a liver iron overload can be performed with visual grading and rSI methods with comparable accuracy, particularly high specificity with good sensitivity. We were able to find the optimal threshold of the rSI method at 10% for liver iron overload detection in the study population. All patients having an rSI of over 10% had hepatic iron overload. Similarly, in visual grading, all patients with a visually detectable liver signal drop (Grades 1–3) were true positive. The detection threshold of rSI corresponds to 63 μmol g^{-1} liver dry weight in the study population (Equation 2), which is at the same level as the 25th percentile of Grade 1 (87 μmol g^{-1}) in visual grading. In our view, this seems to be the sensible detection concentration which could be achieved using the in-phase and out-of-phase methods. This is of clinical interest as 71 μmol g^{-1} liver dry weight has been found to indicate hereditary haemochromatosis, measured from liver biopsies [16]. Also, in haematological malignancies with transfusional iron overload, this detection level might be sufficient in clinical practice as iron accumulates in hepatocytes secondarily after the capacity of the reticuloendothelial system becomes saturated [17]. Interestingly, the detection level of the both methods, visual grading and rSI difference, are consistent with the recently published observation by Alústiza and Castiella [14]. In a recent retrospective study by Lim et al [18], routine in-phase and out-of-phase imaging was found to be of value for detection of significant hepatic siderosis in patients with chronic liver disease. Although they compared iron indexes with a semi-quantitative reference standard, the results are in good agreement with our study.

Table 2. Statistical characteristics of the hepatic iron concentrations of patients in each grade of the visual analyses of both radiologists

Grade	Number of subjects	Median hepatic iron concentration (μmol g^{-1})	25th percentile (μmol g^{-1})	75th percentile (μmol g^{-1})	Range (μmol g^{-1})	Mean hepatic iron concentration (μmol g^{-1})
0	28	32.6	13.7	46.6	9.4–63.8	31.6
1	18	115.0	87.0	140.8	43.8–150.6	109.6
2	22	198.0	187.1	251.6	152.2–325.0	219.3
3	16	318.0	284.5	325.0	270.9–325.0	306.8

Table 3. Contingency table of rSI difference at the 10% threshold

M-HIC	No. of examinations		Total
	No iron overload, rSI <10%	Iron overload, rSI difference ≥10%	
Normal	21	0	21
Overload	5	28	33
Total	26	28	54

M-HIC, MRI-based hepatic iron concentration; rSI, relative signal intensity.

Visual grading was able to differentiate iron overload very accurately at the threshold of 151 μmol g^{-1} with 100% PPV and NPV. Indeed, liver SI, lower than muscle SI, corresponds to iron concentrations above the threshold according to the visual criteria of the Grades 2 and 3 as shown in Table 1. The visual grading analysis was performed accurately and comparably by both of the readers, regardless of their different experience in abdominal radiology. As visual grading does not require any special instrumentation, sequences or calculations made by radiologists, it seems to be relatively easy to introduce and perform. In order to use the criteria successfully, familiarity with the more pronounced susceptibility effect on in-phase and the chemical shift effect on out-of-phase images [13] is essential. Visual grading shows the potential of being a first-hand guideline for radiologists to estimate liver iron content, in addition to more routinely performed liver fat detection.

The correlation of visual grading was better than the correlation of rSI, which did not reach the levels of previously introduced, quantitative methods, for example R_2 or R_2* [19]. The rSI was influenced by the liver fat content, which is shown in false-negative results. Consequently, in the presence of clearly elevated liver fat content, the use of rSI is limited. In these cases the analysis should be made visually using solely in-phase criteria, which was not found to be affected by fatty liver disease in the limited number of patients in this study. In addition to liver fat accumulation, liver oedema might be a potential pitfall, as it decreases the signal on T_1 weighted images [20] and might affect visual grading of the in-phase images. The quantitative range of the standard reference (M-HIC) was limited at 320 μmol g^{-1} liver dry weight. Despite this, the use of M-HIC was justified as a reliable non-invasive measurement of liver concentrations [8] compared with liver biopsies [12]. Liver fat fraction measurement by spectroscopy was not used in this study, although it would have been interesting to evaluate whether these methods were affected by smaller amounts of fatty deposition.

At 1.5 T the echo times of in-phase and out-of-phase images have been virtually constant among the MR scanners of different vendors [13]. We found no significant scanner-specific differences in rSI with a body coil at 1.5 T. The constant echo times enables the general use of the in-phase and out-of-phase methods and also retrospective evaluation of liver iron accumulation at 1.5 T. By contrast, at 3 T there is no consensus on the pair of echoes acquired so these methods cannot be applied directly to 3 T scanners [13].

Conclusions

The accuracy of in-phase and out-of-phase imaging methods of visual grading and rSI to detect liver iron overload was found to be comparable with a high specificity. The optimal threshold for liver iron overload detection was set at an rSI of 10%. The visual grading method was able to distinguish different degrees of iron overload at the threshold of 151 μmol g^{-1} with 100% PPV and NPV with excellent agreement between the readers. Elevated liver fat limits the use of rSI. In these cases, the visual grading from in-phase images is a more preferable method for iron overload evaluation. In-phase and out-of-phase imaging methods do not replace the quantitative R_2 methods, but provide additional information from routine liver MRI at the clinically relevant concentration levels. In the future, the utilisation of the dual-echo approach of in-phase and out-of-phase imaging may increase the number of treatable iron overloaded patients detected.

Acknowledgments

We are very grateful to Saija Hurme, MSC, from the Department of Biostatics, for statistical guidance and Peter B Dean, MD, Professor of Diagnostic Radiology, Turku University, for help in reviewing this paper.

References

1. Brittenham G, Badman D. Noninvasive measurement of iron: report of an NIDDK workshop. Blood 2003;101:15–9.
2. Andrews N. Disorders of iron metabolism. N Engl J Med 1999;341:1986–95.
3. Adams P. Review article: the modern diagnosis and management of haemochromatosis. Aliment Pharmacol Ther 2006;23:1681–91.
4. Alústiza J, Castiella A, De Juan M, Emparanza J, Artetxe J, Uranga M. Iron overload in the liver diagnostic and quantification. Eur J Radiol 2007;61:499–506.
5. Angelucci E, Brittenham G, McLaren C, Ripalti M, Baronciani D, Giardini C, et al. Hepatic iron concentration and total body iron stores in thalassemia major. N Engl J Med 2000;343:327–31.
6. Martin D, Semelka R. Magnetic resonance imaging of the liver: review of techniques and approach to common diseases. Semin Ultrasound CT MR 2005;26:116–31.
7. Wood J. Magnetic resonance imaging measurement of iron overload. Curr Opin Hematol 2007;14:183–90.
8. Gandon Y, Olivié D, Guyader D, Aubé C, Oberti F, Sebille V, et al. Non-invasive assessment of hepatic iron stores by MRI. Lancet 2004;363:357–62.
9. Virtanen J, Komu M, Parkkola R. Quantitative liver iron measurement by magnetic resonance imaging: in vitro and in vivo assessment of the liver to muscle signal intensity and the R2* methods. Magn Reson Imaging 2008;26:1175–82.
10. Alústiza J, Artetxe J, Castiella A, Agirre C, Emparanza J, Otazua P, et al. MR quantification of hepatic iron concentration. Radiology 2004;230:479–84.
11. Olthof A, Sijens P, Kreeftenberg H, Kappert P, van der Jagt E, Oudkerk M. Non-invasive liver iron concentration measurement by MRI: comparison of two validated protocols. Eur J Radiol 2009;71:116–21.
12. Villeneuve J, Bilodeau M, Lepage R, Côté J, Lefebvre M. Variability in hepatic iron concentration measurement from needle-biopsy specimens. J Hepatol 1996;25:172–7.

13. Merkle E, Nelson R. Dual gradient-echo in-phase and opposed-phase hepatic MR imaging: a useful tool for evaluating more than fatty infiltration or fatty sparing. Radiographics 26:1409–18.
14. Alústiza J, Castiella A. Liver fat and iron at in-phase and opposed-phase MR imaging. Radiology 2008;246:641.
15. Borra R, Salo S, Dean K, Lautamäki R, Nuutila P, Komu M, et al. Nonalcoholic fatty liver disease: rapid evaluation of liver fat content with in-phase and out-of-phase MR imaging. Radiology 2009;250:130–6.
16. Kowdley K, Trainer T, Saltzman J, Pedrosa M, Krawitt E, Knox T, et al. Utility of hepatic iron index in American patients with hereditary hemochromatosis: a multicenter study. Gastroenterology 1997;113:1270–7.
17. Stark D. Hepatic iron overload: paramagnetic pathology. Radiology 1991;179:333–5.
18. Lim R, Tuvia K, Hajdu C, Losada M, Gupta R, Parikh T, et al. Quantification of hepatic iron deposition in patients with liver disease: Comparison of chemical shift imaging with single-echo T_2*-weighted imaging. AJR AM J Roentgenol 2010;194:1288–95.
19. Wood J, Enriquez C, Ghugre N, Tyzka J, Carson S, Nelson M, et al. MRI R2 and R2* mapping accurately estima hepatic iron concentration in transfusion-dependent thalassemia and sickle cell disease patients. Blood 2005;106:1460–5.
20. Noone T, Semelka R, Siegelman E, Balci N, Hussain S, Kim P, et al. Budd-Chiari syndrome: spectrum of appearances of acute, subacute, and chronic disease with magnetic resonance imaging. J Magn Reson Imaging 2000;11:44–50.